Physics – Uspekhi **50** (1) 37 – 51 (2007)

REVIEWS OF TOPICAL PROBLEMS PACS numbers: 03.65.Ge, 03.65.Sq, 42.25.Bs, 42.25.Gy

Tunneling of electromagnetic waves: paradoxes and prospects

A B Shvartsburg

DOI: 10.1070/PU2007v050n01ABEH006148

Contents

Abstract. Electromagnetic wave tunneling through photonic barriers and effects of frustrated total internal reflection (FTIR) are considered for waves of different spectral regions. The discovered effects of nonlocal dispersion of gradient dielectric barriers, wherein the spatial permittivity profile $\varepsilon(z)$ determines the cutoff frequency that depends on the shape and geometric parameters of this profile are shown to play the decisive role in wave tunneling through nonuniform barriers. Special emphasis is placed on the effects of total wave transmission at frequencies lower than the cutoff frequency in the FTIR mode (reflection-free tunneling) characteristic of gradient media. The generality of these effects for a broad wave spectrum is illustrated using exact analytic solutions of the Maxwell equations describing wave tunneling through nonuniform transparent dielectrics. Also discussed are controversial issues surrounding the FTIR theory and the prospects for using gradient photonic barriers for the development of thin-film filters and polarizers, efficient reflectors, and reflection-free coatings.

1. Introduction. Hartman's paradox

Tunneling is a fundamental phenomenon in the dynamics of waves of various physical natures. The interest in it was aroused after Gamow's famous work (1928) dedicated to nuclear alpha decay [1], where the probability that an alpha particle with energy E escapes a potential barrier with a height U_0 for $E < U_0$ was determined by precisely the tunneling. Three years after this first application of quantum mechanics to nuclear physics, Condon's calculation [2] of the velocity or transit time of a particle in the domain $E < U_0$ attempted in the framework of the new theory revealed a basic problem: How to define these quantities in the 'classically forbidden' zone, where the particle momentum should be assigned imaginary values. A year later, MacColl [3] arrived at the conclusion that "there is no appreciable delay in the transmission of the (wave — E.N.R) packet through the barrier." The question remained open, but in the subsequent three decades, the probabilities of particle tunneling through different types of potential barriers were derived in many 'hot' problems of spectroscopy, atomic collision theory, and solid-state physics; in the light of these successes, the thirty-year old problem receded into the background.

The interest in this problem was rekindled after Hartman's work, dated 1962, in which the time of tunneling through a barrier for a particle with energy E was determined from the phase of the complex barrier transmission function $T = |T| \exp(\mathrm{i}\phi)$ with the help of the general formula [4]

$$\tau_\mathrm{p} = \hbar \frac{\partial \phi}{\partial E} . \tag{1.1}$$

Using the well-known expression for the transmission function of a mass m tunneling through a potential barrier of height U_0 and width d (Fig. 1),

$$|T| \propto \exp(-\aleph d) , \quad \phi = \arctan\left[\frac{(2 - U_0/E)\tanh(\aleph d)}{2\sqrt{U_0/E - 1}}\right],$$

$$\aleph = \frac{\sqrt{2m(U_0 - E)}}{\hbar} , \tag{1.2}$$

and considering a wide barrier ($\aleph d \gg 1$), Hartman has shown that (1.1) leads to the simple formula [5]

$$\tau_\mathrm{p} = \frac{\hbar}{\sqrt{E(U_0 - E)}} . \tag{1.3}$$

This result indicated unexpected properties of the tunneling 'phase time' τ_p in (1.1):

(i) the time τ_p depends on the energy of a tunneling particle but is independent of its mass;

A.B. Shvartsburg Scientific and Technological Center for Unique Instrumentation, Russian Academy of Sciences,
ul. Butlerova 15, 117342 Moscow, Russian Federation
Tel. (7-495) 333 61 02
E-mail: alexshvarts@mtu-net.ru

Received 14 June 2006, revised 21 July 2006
Uspekhi Fizicheskikh Nauk **177** (1) 43 – 58 (2007)
Translated by E N Ragozin; edited by A M Semikhatov

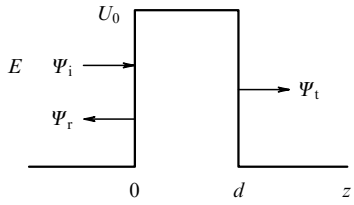

Figure 1. Tunneling of a particle with energy E across a rectangular potential barrier of a height $U_0 > E$ and width d; the wave functions Ψ_i, Ψ_r, and Ψ_t correspond to the incident, reflected, and transmitted particles.

(ii) the time τ_p is minimal at $E = 0.5U_0$; in this case, $\tau_p = \hbar/E$ and $\tau_p = \hbar/E$; and

(iii) the time τ_p is independent of the tunneling path; for a sufficiently long path, the particle speed V could reach supraluminal values $V > c$.

The last conclusion is referred to as 'Hartman's paradox' in the literature. This paradox, which was derived from standard formulas (1.2) given in many textbooks and which invokes no additional hypotheses, raised lively debate, which is ongoing [6–12]. However, direct measurement of the time of electron tunneling through quantum barriers has proved to be an intricate task, and the idea was conceived of verifying Hartman's conclusions in the classical effects of electromagnetic wave tunneling through macroscopic photonic barriers. This idea relied on the formal similarity between the stationary Schrödinger equation and the Helmholtz equation; the tunneling of particles through a forbidden zone was compared to the passage of an electromagnetic (EM) wave through a dispersive medium, for instance, a plasma layer whose plasma frequency Ω_{pl} is higher than the wave frequency ω.

We introduce the imaginary refractive index n of this medium as

$$n = iN_-\,, \quad N_- = \sqrt{u^2 - 1}\,, \quad u = \frac{\Omega_{pl}}{\omega} > 1\,, \tag{1.4}$$

and consider the model problem of the normal incidence on a plasma layer of thickness d to find the modulus and phase of the complex transmission function T from the field continuity conditions at the boundaries as

$$|T| = \frac{2N_-}{\sqrt{(1 - N_-^2)\sinh^2(pd) + 4N_-^2\cosh^2(pd)}}\,,$$

$$\tan\phi = \frac{(1 - N_-^2)\tanh(pd)}{2N_-}\,, \quad p = \frac{\omega N_-}{c}\,. \tag{1.5}$$

The wave phase in (1.5), defined by the discontinuity of the incident and tunneling wave fields at the boundary $z = 0$, does not increase proportionally with the path length d and tends to a constant value at the output from a 'thick' layer ($pd \gg 1$); a similar 'saturation' of the wave function phase also follows from expression (1.2). By defining the phase time τ as the time of group delay [4], we obtain a formula similar to (1.1) and the limit expression for the 'thick' layer:

$$\tau_p = \frac{\partial\phi}{\partial\omega}\,, \quad \tau_p\Big|_{pd \gg 1} = \frac{2}{\omega N_-}\,. \tag{1.6}$$

The second formula in (1.6) is the analog of Hartman's paradox for an electromagnetic wave. In contrast to the total internal reflection of the wave from an opaque half-space, the partial reflection from an opaque barrier of finite width has come to be known as frustrated total internal reflection (FTIR). The time of wave tunneling through a wide photonic barrier ($pd \gg 1$) turned out to be independent of the barrier width, once again bringing up the question of supraluminal speed under FTIR conditions.

In subsequent years, the progress of pulsed radiophysics and quantum optics fostered new experiments involving FTIR, which were concurrently pursued in the optical and microwave ranges. The tunneling of the fundamental mode of a metal radio waveguide through a section with a lower cutoff frequency [13–17], the transmission of light through a multilayer filter [18], and an optical fiber with built-in Bragg gratings [19] were interpreted in the framework of the concept of complex time τ [20], with $\mathrm{Re}\,\tau = \tau_p$ given by formula (1.1), and the tunneling time was defined in Buttiker's works [21, 22] in terms of the transmission function $T = |T|\exp(i\phi)$ as

$$\tau_{Bu} = \sqrt{\tau_p^2 + \tau_T^2}\,; \quad \tau_T = \frac{\partial \ln|T|}{\partial\omega}\,. \tag{1.7}$$

Using (1.7) to calculate the time τ_p for plasma layer (1.5), we obtain $\tau_{Bu} = t_0/N_-$, $t_0 = d/c$ for a large layer width ($pd \gg 1$). With this definition, the time τ_{Bu} is proportional to the path length d but may turn out to be either longer or shorter than the 'light time' t_0, depending on the frequency.

Measurements of the time delay for the fundamental TE_{01} waveguide mode near the cutoff frequency [23] showed that each of the quantities (1.1) and (1.7) approaches the measurement data only in some frequency intervals. To interpret the measurements in Ref. [22], the authors of [24] and [25] proposed another theory, which treated the tunneling as stochastic particle motion in the forbidden zone related to multiple reflections from the zone boundaries and described by the imaginary-time equation of telegraphy [26].

The tunneling time problem became even more acute after experiments with two wave barriers between which the wave propagates freely ('generalized Hartman's paradox'). For microwaves with a frequency ω, the time τ_p of propagation along a waveguide path with a cutoff frequency $\Omega < \omega$ containing two 'opaque' sections with $\Omega_1 > \omega$ spaced at a distance D turned out to be independent of D [27]. A similar effect was noted in Ref. [28] for IR pulses in an optical fiber with two photonic barriers formed by fiber lengths with the spatially modulated refractive index

$$n(z) = n_0\big[1 + n_1\cos(Kz)\big]\,, \quad n_1 \ll n_0\,.$$

This barrier (the grating drawn inside the light guide) was responsible for waves with frequencies close to the Bragg frequency $\omega_B = cK/2n_0$; the tunneling time, which was estimated from the arrival time of the pulse peak, corresponded to supraluminal speeds.

These shifts in the peak of the pulse in the FTIR regime, which were also observed in Refs [17, 28, 29], were attributed to the deformation of the pulse envelope in the interference of the forward and backward waves; this deformation is responsible for the suppression of the pulse 'tail,' which is registered as an acceleration of its peak. Unlike the acceleration of the peak in a stationary medium, a similar effect in an amplifying medium was attributed in Refs [30, 31] to the nonuniformity of amplification: the energy of the medium was transferred primarily to the head part of the pulse, while

the energy gain in the 'tail' of the pulse was reduced due to saturation.

In investigating the occurrence of supraluminal speeds in wave processes, the authors of the above papers emphasize that these results do not contradict the relativistic causality: the speed V of a signal in a stationary medium treated as the propagation speed of the field discontinuity remains bounded: $V \leqslant c$; however, this speed has never been measured because this would require a detector with infinite sensitivity [32]. A formulation of the causality principle with the tunneling effects included was then proposed in Refs [13, 17]: at any instant, the energy flux at the output of a stationary medium cannot exceed the flux that would have existed in its absence. This formulation, like the FTIR paradoxes, evokes mutually contradictory estimates [33, 36].

But the processes of wave tunneling attract attention not only because of their uncommonness but also due to the prospect of using them to solve problems of condensed-matter physics [37], magnetic hydrodynamics [38], quantum optics [39], and photonic crystals [40], and, in particular, to make artificial materials nonexistent in nature [41]. Research in the new areas related to the propagation of electromagnetic waves in dielectric media with a smooth in-medium variation of the refractive index is underway in gradient optics [42, 43]. Special emphasis is here placed on the wave reflection and transmission by thin nonuniform material layers with layer thicknesses and nonuniformity scale lengths comparable to the wavelength [44]. The synthesis of suchlike layered structures is now a rapidly developing area in nanotechnology [45, 46].

The physical foundations of these processes consist in the special mechanism of wave dispersion in nonuniform dielectrics. We emphasize the fundamental difference between this mechanism and the material dispersion related to the parameter $\partial^2 n/\partial\omega^2$, as well as the spatial dispersion of uniform media: the latter, as is well known from crystal optics and plasma physics [47], leads to small corrections to the refractive index of the order of $a/\lambda \ll 1$, where a is the lattice spacing or the particle mean free path in the medium and λ is the wavelength. Away from the resonance frequencies of the medium, these effects are slowly accumulated along the wave propagation path over distances comprising many wavelengths. By contrast, gradient media are characterized by the inverse ratio between the nonuniformity scale length d and the wavelength: $\lambda \leqslant d$. The evolution of waves in such media has several special features.

1. The wave dispersion in a gradient layer depends not only on the nonuniformity scale length but also on the gradient and curvature of the spatial profile of n. The effects of this nonlocal dispersion, being accumulated over a distance of the order of a wavelength, may radically change the reflection and transmission spectra of the layer. For instance, in a weakly dispersive material layer, they may give rise to a cutoff frequency Ω controlled by nonuniformity parameters [48] and to the FTIR mode for the frequencies $\omega < \Omega$.

2. Wave tunneling through a one-dimensional nonuniform medium with a refractive index $n(z)$ is possible not only in the domain $n^2 < 0$ but also in the domain $n^2 > 0$, $\mathrm{d}n^2/\mathrm{d}z < 0$. This effect is indicative of the FTIR mode for EM waves in a broad spectral range.

3. For a given spectral range, it is possible to choose a material and a profile $n(z)$ such that the nonlocal dispersion effects are concentrated in a frequency band away from the material absorption bands. The wave dynamics in such media are described by exact analytic solutions of the Maxwell equations, which are constructed without any assumptions regarding the smallness or slowness of the variation in the parameters of the medium or the field.

The present review is concerned with optimization of EM wave energy transfer through gradient media in the tunneling mode. The present-day interest in the physical principles and mathematical foundations of this process is stimulated by several 'hot' problems:

(i) to specify the total transmission conditions for waves of various physical natures tunneling through nonuniform wave barriers;

(ii) to find the amplitude, phase structure, and polarization of waves of the optical and radio ranges in spatially distributed FTIR systems; and

(iii) to present exactly solvable multiparameter models for the optimization of energy transfer in thin gradient layers.

The review is organized as follows: Section 2 is dedicated to the conventional scheme of FTIR observation employing the Goos–Hanchen effect in a system of two prisms. An exactly solvable model of wave tunneling through a photonic barrier with a concave profile of the refractive index is described in Section 3; discussed with the help of this model in Section 4 is the mode of reflection-free tunneling. Sections 5 and 6 are concerned with the generalizations of these effects for a waveguide with a nonuniform diaphragm and for transmission lines with continuously distributed parameters. In contrast to Sections 3–6, which are concerned with the bulk effects of FTIR, considered in Section 7 are surface waves in gradient media. Several features of wave tunneling through curvilinear, absorbing, and transient photonic barriers are mentioned in the conclusion.

2. Uniform photonic barriers

This section is concerned with electromagnetic wave tunneling under conditions of frustrated total internal reflection. This problem is considered for a simple configuration: two isosceles transparent prisms made of a material with a refractive index n, with the long sides of the prisms facing each other (Fig. 2); these sides are parallel and spaced at a distance d. The absorption and frequency dispersion in the prism material are neglected. The air gap between the prisms makes up a uniform photonic barrier for waves incident on the $z = 0$ gap boundary at an angle θ that exceeds the total internal reflection angle $\theta_{\mathrm{cr}} = \arcsin(1/n)$. The incident beam is partly reflected and partly tunnels through the barrier to shift by a distance l and find itself in the right prism. This scheme, which attracts attention in the analysis of tunneling effects in radiophysics and optics [49, 50], permits obtaining:

a) lengthening of the tunnel path at oblique incidence;

b) a broad frequency range of the waves that tunnel through the barrier without dispersion; and

c) the birefringence of obliquely incident waves in FTIR.

For simplicity of calculations, we can conveniently begin analyzing the problem with the case of S-polarized waves; in the geometry under consideration, they are characterized by the electric field component E_x and the magnetic field components H_y and H_z. The analysis comprises several stages:

(i) calculation of the complex transmission function and the phase time of transit through the barrier;

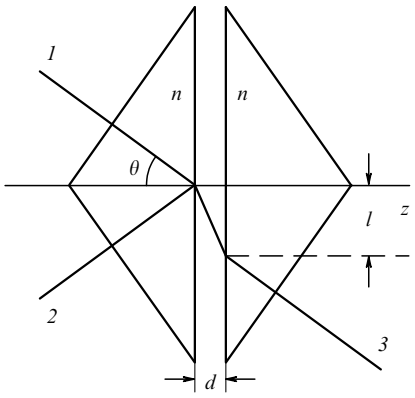

Figure 2. Frustrated total internal wave reflection: incident *1*, reflected *2*, and tunneling *3* waves and Goos–Hanchen shift *l* in the system of two prisms separated by a distance *d*.

(ii) determination of the group velocity of waves and the group delay time inside the barrier; and

(iii) determination of the transverse shift of rays in the FTIR.

All these quantities depend on the amplitude and phase structure of the field inside the barrier, formed in the interference of the incident and reflected waves in the opacity domain $0 \leqslant z \leqslant d$. To analyze this structure, we can conveniently use the set of formulas for the field components derived from the Maxwell equations for a plane wave with the continuity of the fields at the boundaries $z = 0$ and $z = d$ taken into account:

$$
\begin{aligned}
&E_x = E_i M\left[\exp(-pz) + Q\exp(pz)\right],\\
&H_z = -nE_x \sin\theta\,, \quad p = \frac{\omega}{c}\, f,\\
&H_y = \mathrm{i} f E_i M\left[\exp(-pz) - Q\exp(pz)\right],\\
&Q = \frac{(f + \mathrm{i}n\cos\theta)\,\exp(-2pd)}{f - \mathrm{i}n\cos\theta}\,,\\
&M = \frac{1+R}{1+Q}\,, \quad f = \sqrt{n^2\sin^2\theta - 1}\,.
\end{aligned}
\tag{2.1}
$$

Here, E_i is the amplitude of the electric field incident on the boundary $z = 0$ and R_S is the complex reflection coefficient:

$$
R_S = \frac{\tanh(pd)\,(n^2-1)}{\tanh(pd)\,A + 2inf\cos\theta}\,, \quad A = n^2\cos^2\theta - f^2\,. \tag{2.2}
$$

Using formulas (2.1) and (2.2), it is possible to fulfill stages (i)–(iii) of the analysis planned above:

1. On finding the field E_x in the plane $z = d$, we determine the amplitude and phase of the complex transmission function $T_S = |T|\exp(\mathrm{i}\phi_S)$:

$$
|T| = \frac{2fn\cos\theta}{\cosh(pd)\sqrt{(2nf\cos\theta)^2 + t^2A^2}}\,, \quad t = \tanh(pd)\,, \tag{2.3}
$$

$$
\phi_S = \arctan\left(\frac{tA}{2nf\cos\theta}\right). \tag{2.4}
$$

Introducing the characteristic length $d_{cr} = c/\omega f$, we can show that in tunneling over a long distance ($d \gg d_{cr}$), the energy flux decreases as $|T|^2 \approx \exp(-2d/d_{cr})$ and the phase 'saturates,' approaching a constant value independent of the distance. The temporal FTIR characteristics are conveniently expressed in terms of t_0, the time of light propagation over a distance d. The 'phase time' τ_S calculated in accordance with formula (1.1) is

$$
\frac{\tau_S}{t_0} = \frac{2nf^2A\cos\theta(1-t^2)}{(2nf\cos\theta)^2 + t^2A^2}\,, \quad t_0 = \frac{d}{c}\,. \tag{2.5}
$$

2. We next consider the group delay time t_g related to the group velocity v_g of the tunneling wave. The velocity v_g is defined by the energy flux P and the energy density W [51]:

$$
v_g = \frac{\mathbf{P}}{W}\,, \quad P = \frac{c\mathbf{E}\times\mathbf{H}^*}{4\pi}\,, \quad W = \frac{|\mathbf{E}|^2 + |\mathbf{H}|^2}{8\pi}\,. \tag{2.6}
$$

We substitute field components (2.1) in expression (2.6) and find the velocity components v_{gz} and v_{gy}:

$$
\begin{aligned}
&v_{gz} = \frac{2nf^2\cos\theta}{\Delta}\,,\\
&v_{gy} = \frac{n\sin\theta\left\{(n^2-1)\cosh\left[2p(d-z)\right] - A\right\}}{\Delta}\,,\\
&\Delta = n^2\sin^2\theta(n^2-1)\cosh\left[2p(d-z)\right] - A\,.
\end{aligned}
\tag{2.7}
$$

The quantity A is defined in (2.2). As is evident from formulas (2.7), the group velocity of a wave tunneling through a uniform gap is not constant and depends on the z coordinate. The group delay t_{gS} is found by integrating the expression $\mathrm{d}t_g = \mathrm{d}z/v_{gz}$ from $z = 0$ to $z = d$:

$$
\frac{t_{gS}}{t_0} = \left[\frac{n^2\sin^2\theta(n^2-1)\sinh(2pd)}{2pd} - A\right]\frac{1}{2nf^2\cos\theta}\,. \tag{2.8}
$$

3. The transverse ray shift in FTIR (the Goos–Hanchen shift) is defined by the ray trajectory equation in the (y, z) plane:

$$
\frac{\mathrm{d}z}{v_{gz}} = \frac{\mathrm{d}y}{v_{gy}}\,. \tag{2.9}
$$

We integrate Eqn (2.9) to obtain the shift at the plane $z = d$ for an S-polarized beam passing through the point $y = 0$, $z = 0$:

$$
l_S = \frac{d\sin\theta}{2f^2\cos\theta}\left[-A + \frac{(n^2-1)\sinh(2pd)}{2pd}\right]. \tag{2.10}
$$

Following the above scheme, it is also possible to investigate the tunneling of P-polarized waves [52]. In particular, the amplitude and phase of the transmission function for the P-wave is given by formulas (2.3) and (2.4) with A replaced by

$$
B = \cos^2\theta - n^2f^2\,. \tag{2.11}
$$

The same replacement in formula (2.5) leads to an expression for the phase time τ_P. Formulas for the group delay t_{gP} and the transverse shift l_P in the field of P-waves follow from expressions (2.8) and (2.10) when A is replaced by B and $n^2 - 1$ by $n^2f^2 + \cos^2\theta$.

We now highlight several FTIR features for a rectangular barrier.

1. We first discuss the FTIR for the S-waves. The dependence $\tau = \tau(d)$ of the time τ in (2.5) on the distance is nonmonotonic: for a narrow gap ($d \ll d_{cr}$), the time τ increases proportionally to the gap width d. At $d = d_{max} = 0.775 d_{cr}$, τ reaches its peak; on further gap broadening, τ begins to decrease and decays as $\exp(-2d/d_{cr})$ for $d \gg d_{cr}$. Therefore, applying formula (1.1) to the FTIR problem accentuates Hartman's paradox about the barrier-width-independent tunneling time: for very wide barriers ($d \gg d_{cr}$), the tunneling time tends to shorten. When the dependence of τ_S on d is represented in the plane of dimensionless variables τ/t_0 and d/d_{cr}, it can be seen that the quantity τ_S takes supraluminal values $\tau_S < t_0$ in a broad range of parameters n, θ, and d (Fig. 3a, curve *1*).

2. Another unexpected corollary of formula (2.5) consists in the emergence of the domain of negative values of the phase time for large incidence angles ($\theta > \theta_{S,P}$) [53]; for S(P)-waves, the angles $\theta_{S,P}$ are determined from the conditions $A = 0$ ($B = 0$):

$$\theta_S = \frac{1}{2}\arccos\left(-\frac{1}{n^2}\right), \quad \theta_P = \arcsin\sqrt{\frac{n^2+1}{n^4+1}}. \qquad (2.12)$$

For glass ($n = 1.5$), we obtain $\theta_S = 58^\circ$ and $\theta_P = 47^\circ$ from formulas (2.12). Figure 3a shows the $\tau < 0$ domains for the S- and P-waves. Regarding τ as the tunneling time, several authors [54, 55] relate the values $\tau < 0$ to a negative tunneling velocity.

The emergence of supraluminal and negative tunneling velocities in the FTIR theory initiated a debate between the proponents of mutually antithetic concepts in this theory. In particular, in Refs [56, 57] dedicated to the tunneling of narrow localized Gaussian wave packets, the situation with $\tau < 0$ is interpreted as a result of a rapid reduction in the probability density flux in the interference of the incident wave and the wave reflected from the front side of the barrier.

3. In the framework of an alternative concept [52, 58], the tunneling time t_g is defined in terms of the group velocity (2.8) of waves inside the barrier. When this approach is adopted, the above paradoxes do not emerge: the time t_g is positive and the tunneling is a slow process ($t_g > t_0$) (Fig. 3b). The barrier transmittance for S-waves is higher than for P-waves (Fig. 3c).

4. We also note the birefringence of waves in the FTIR mode, which is responsible for different transverse beam shifts (the Goos–Hanchen effect) for S- and P-waves in (2.10). This birefringence is characteristic of precisely the tunneling waves. In the transmission band for a plane-parallel layer, this effect degenerates: $l_S = l_P$; this equality also occurs in the case of FTIR at the incidence angle θ_0 defined by the equation

$$\frac{\sinh(2pd)}{2pd} = \frac{(n^2-1)\sin^2\theta_0}{2-(n^2+1)\sin^2\theta_0}. \qquad (2.13)$$

As is evident from Fig. 3d, the shifts $l_{S,P}$ are equal to several wavelengths for $d \approx d_{cr}$. It is difficult to measure the above shifts in the visible range; however, the Goos–Hanchen effect was recorded for centimeter radio waves tunneling (in the geometry of Fig. 1) through a gap between two paraffin prisms; for the gap width $d = 1-10$ cm, the shift l was equal to 2–4 cm [49].

5. Formulas (2.3) and (2.4) for the complex transmission function T of a layer in the FTIR mode ($\theta > \theta_{cr}$) transform

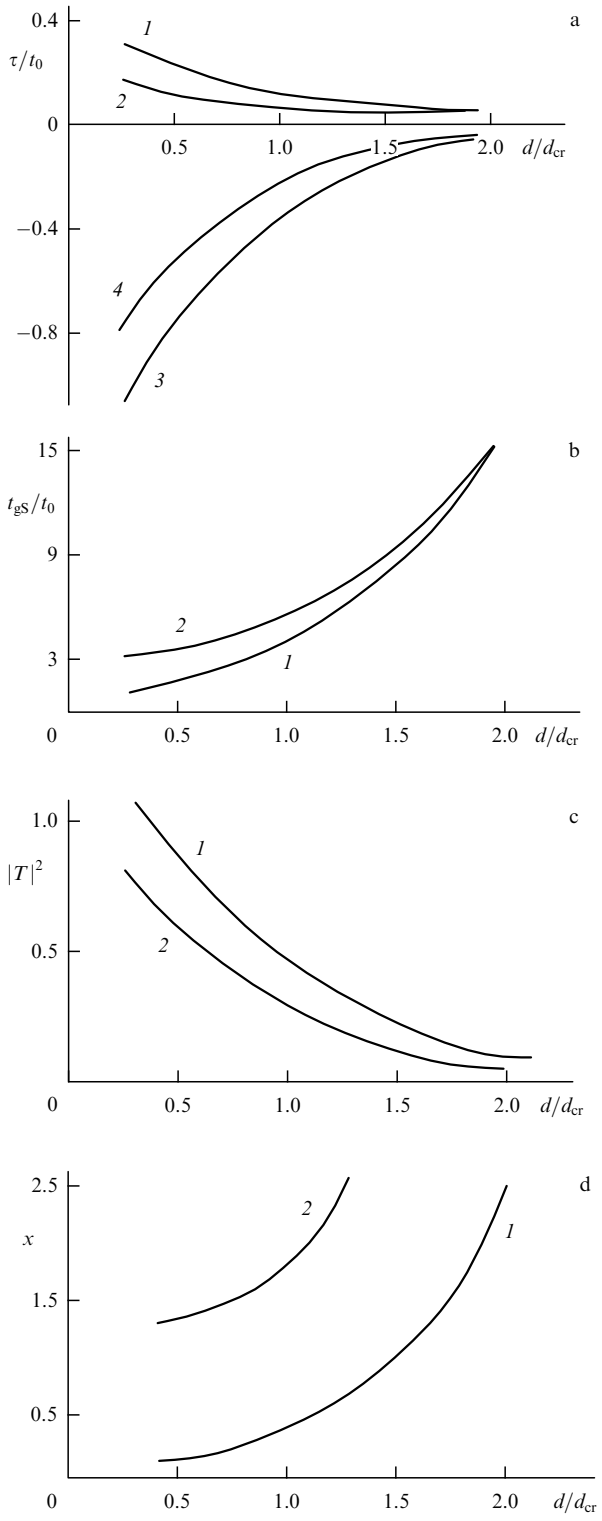

Figure 3. Dependence of polarization effects in the wave tunneling through a system of two prisms (see Fig. 2) on the normalized gap width d/d_{cr}, $d_{cr} = c/f\omega$, $n = 1.5$: (a) supraluminal (curves *1* and *2*) and negative (curves *3* and *4*) values of the phase time $\tau_S(\tau_P)$ for S(P)-waves calculated in accordance with formula (1.1); curves *1*–*4* are plotted for the respective incidence angles $\theta = 50^\circ$, 30°, 75°, and 60°; (b) normalized subluminal time t_{gS}/t_0 in (2.8); curves *1* ($\theta = 50^\circ$) and *2* ($\theta = 60^\circ$) are plotted for the S- and P-waves, respectively; (c) transmission coefficient $|T|^2$ for S- and P-waves (curves *1* and *2*) under the conditions of Fig. 3b; (d) normalized transverse shift of the tunneling waves l ($x = l/\lambda f$, λ is the wavelength) for S- and P-waves (curves *1* and *2*) under the conditions of Fig. 3b.

into the well-known expressions for T in the transmission band ($\theta < \theta_{cr}$) when f is replaced by $-if_1$, $f_1 = \sqrt{1 - n^2 \sin^2\theta}$, and $\tanh(d/d_{cr})$ is replaced by $-i\tan(d/d_1)$, $d_1 = \omega f_1/c$ [51].

In the problem considered above, the FTIR mode emerges in the conventional scheme involving oblique wave propagation between media with $n > 1$ through a uniform barrier with $n = 1$. Similar effects are also manifested in the opposite case: at normal wave incidence from the air ($n = 1$) onto a medium with a varying $n > 1$ when the refractive index in this medium decreases in accordance with some law $n(z)$. Wave tunneling through this nonuniform barrier is discussed in Section 3.

3. Gradient photonic barriers (exactly solvable model)

The problems of wave propagation through media with a continuous spatial variation of the refractive index constitute a vast realm of mathematical physics. This section is concerned with one of these problem, the optics of gradient media. Such media are characterized by a unidirectional gradient of the refractive index. By adopting this direction as the z axis, we can represent their permittivity as

$$\varepsilon(z) = n_0^2 U^2(z)\,, \quad U(0) = 1\,, \tag{3.1}$$

where n_0 is the value of the refractive index at the $z = 0$ boundary of the medium and U is some twice-differentiable dimensionless function, which defines the spatial profile of the refractive index; the medium material dispersion $n_0(\omega)$ and the wave absorption are neglected. We consider the propagation of an EM wave normally incident from a vacuum onto the $z = 0$ boundary in the z-direction; the wave field components E_x and H_y can then be expressed in terms of an auxiliary function Ψ [51]:

$$E_x = -\frac{1}{c}\frac{\partial\Psi}{\partial t}\,, \quad H_y = \frac{\partial\Psi}{\partial z}\,. \tag{3.2}$$

The function Ψ is determined by the wave equation that follows from the Maxwell equations:

$$\frac{\partial^2\Psi}{\partial z^2} - \frac{n_0^2 U^2(z)}{c^2}\frac{\partial^2\Psi}{\partial t^2} = 0\,. \tag{3.3}$$

The EM-wave reflection and transmission by a gradient dielectric barrier of finite width depends on the nonlocal dispersion defined by the $U(z)$ profile shape and the barrier width d. To represent this dependence in explicit form, we must use a flexible $U(z)$ model that admits an exact solution of Eqn (3.3) without any assumptions about the smallness or slowness of the variation of the fields and medium parameters. Exactly solvable models known in the electrodynamics of stratified media describe a monotonic dependence $U^2(z)$ on one parameter, the characteristic length L [43]:

$$U^2 = \left(1 + \frac{z}{L}\right)^{-2}, \quad U^2 = \left(1 + \frac{z}{L}\right), \quad U^2 = \left(1 + \frac{z}{L}\right)^{-1}.$$

We here use a more flexible U^2 model [59] with two free parameters L_1 and L_2, which represents a concave profile of the refractive index (Fig. 4)

$$U(z) = \left(1 + \frac{z}{L_1} - \frac{z^2}{L_2^2}\right)^{-1}. \tag{3.4}$$

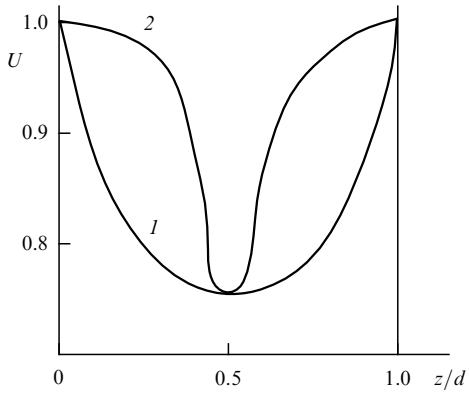

Figure 4. Normalized refractive-index profiles of different shapes $U(z)$ having the same width $d = 80$ mm and modulation depth $n_{min} = 0.75n_0$: *1*— profile (3.4), $y^2 = 1/3$; *2* — profile (5.1), $M = 0.1$, $g = 0.025$.

The characteristic lengths L_1 and L_2 are related to the profile minimum u_{min} and the barrier width d as

$$U_{min} = (1 + y^2)^{-1}, \quad L_2 = \frac{d}{2y}, \quad L_1 = \frac{d}{4y^2}\,, \quad y = \frac{L_2}{2L_1}\,. \tag{3.5}$$

The exact solution of inhomogeneous wave equation (3.3) for a monochromatic wave inside barrier (3.4) can be written as the sum of the forward and backward waves:

$$\Psi = \frac{\left[\exp(i q\eta) + Q\exp(-i q\eta)\right]\,\exp(-i\omega t)}{\sqrt{U(z)}}\,. \tag{3.6}$$

The dimensionless quantity Q, to be determined from the field continuity conditions at the rear boundary of the barrier $z = d$, is the backward wave contribution to the field inside the barrier, and the variable η is the phase path length:

$$Q = -\frac{(1 - i\gamma/2 - n_0 N)\,\exp(2iq\eta_0)}{(1 - i\gamma/2 + n_0 N)}\,,$$
$$\gamma = (kL_1)^{-1}, \quad k = \frac{\omega}{c}\,, \tag{3.7}$$

$$\eta(z) = \int_0^z U(x)\,dx = \frac{L_2}{2\sqrt{1+y^2}}\ln\left(\frac{1 + zy_+/L_2}{1 - zy_-/L_2}\right), \tag{3.8}$$
$$\eta_0 = \eta(d) = \frac{L_2}{\sqrt{1+y^2}}\ln\left(\frac{y_+}{y_-}\right), \quad y_\pm = \sqrt{1+y^2} \pm y\,.$$

Formula (3.6) represents the field Ψ in the form of an amplitude-modulated wave in the phase plane (η, t). The propagation regime of this wave is determined by the wavenumber q:

$$q = kn_0 N\,, \quad N^2 = 1 - u^2\,, \quad u = \frac{\Omega}{\omega}\,, \quad \Omega = \frac{2cy\sqrt{1+y^2}}{dn_0}\,. \tag{3.9}$$

The frequency dependence of the wavenumber (dispersion) is described by a waveguide-type formula, with the quantity Ω in (3.9) playing the role of the cutoff frequency. We emphasize that the emergence of the critical frequency in a nonuniform barrier is due not to the properties of the barrier material but to geometric parameters, the barrier shape $U(z)$

and width d. When the nonuniformity effects subside (L_1, $L_2 \to \infty$), this nonlocal dispersion becomes weaker, the cutoff frequency decreases to zero, and formula (3.9) for the wavenumber takes the standard form $q = kn_0$.

The nonlocal barrier dispersion separates the high-frequency domain ($u < 1$, $N^2 > 0$), which corresponds to the propagation mode, from the low-frequency domain ($u > 1$, $N^2 < 0$), which is associated with the tunneling mode. This mode is considered below in the course of solving wave equation (3.6); the function Ψ_t for the tunneling field can be obtained from Ψ in (3.6) by the substitution $q \to ip$, $N \to iN_-$ with $N_- = \sqrt{u^2 - 1}$:

$$\Psi_t = \frac{\left[\exp(-p\eta) + Q_0 \exp(p\eta)\right] \exp(-i\omega t)}{\sqrt{U(z)}},$$

$$Q_0 = \left(n_0 N_- + \frac{\gamma}{2} + i\right) \exp(-2p\eta_0) \left(n_0 N_- - \frac{\gamma}{2} - i\right)^{-1}. \quad (3.10)$$

The quantity Q_0 follows from Q in (3.7) upon the same substitution. We substitute expression (3.10) in Eqns (3.2) to obtain the field components E_x and H_y inside the barrier in the FTIR mode. The conditions for the continuity of these components at the barrier boundaries give explicit expressions for the reflection coefficient R and the transmission function T.

The solution under discussion describes the simple case of FTIR in a solitary photonic barrier. To optimize these effects, we consider tunneling through a system of m similar adjacent layers described by Eqn (3.4). Using the continuity conditions for the fields at the interfaces between neighboring layers, it is possible to find the field in each layer; assigning the number $m = 1$ to the layer at the distant side of the system, we obtain a simple recursive formula for the parameter Q_m corresponding to the mth layer ($m \geqslant 1$):

$$Q_m = Q_0 \exp\left[-2p(m-1)\eta_0\right]. \quad (3.11)$$

The quantity Q_0 is defined in (3.10).

The reflection coefficient of the FTIR system under discussion is found from formula (3.11) and the continuity conditions at $z = 0$:

$$R = \frac{1 + iG}{1 - iG}, \quad G = \frac{\gamma}{2} - n_1 \frac{1 - Q_m}{1 + Q_m}, \quad n_1 = n_0 N_-. \quad (3.12)$$

Substituting formula (3.11) in expression (3.12), we finally obtain [48]

$$R = \frac{t_m(1 + \gamma^2/4 + n_1^2) - \gamma n_1}{t_m(1 - \gamma^2/4 - n_1^2) + \gamma n_1 + i(2n_1 - \gamma t_m)},$$

$$t_m = \tanh(mp\eta_0). \quad (3.13)$$

The modulus of the complex transmission function $T = |T| \exp(i\phi_t)$ is related to $|R|^2$ by the conservation law:

$$|T|^2 = 1 - |R|^2, \quad (3.14)$$

where the phase ϕ_t is

$$\phi_t = \arctan\left[\frac{t_m(1 - \gamma^2/4 - n_1^2) + \gamma n_1}{2n_1 - \gamma t_m}\right]. \quad (3.15)$$

As in the case of rectangular barrier (2.4), the phase shift of a tunneling wave does not accumulate in the course of propagation but is formed at the boundary. With an increase in the number of barriers ($m \gg 1$, $t_m \to 1$), the modulus of the transmission function decreases in accordance with the law $\exp(-2mp\eta_0)$; as $t_m \to 1$, it is clear from formula (3.15) that the phase tends to a constant value ϕ_m independent of the number of barriers (Fig. 5, curve *1*). The 'phase time' τ calculated from (1.6) also tends to a constant value with increasing m (Fig. 5, curve *2*). In this case, in the system of nonuniform photonic barriers, there again emerges Hartman's paradox: the tunneling velocity $v = md/\tau$ must increase with the barrier width md to attain the value $m = 10$ at $v = c$; the subsequent increase in m should lead to supraluminal values ($v > c$). Moreover, a 'negative tunneling time' $\tau < 0$ may emerge near the cutoff frequency [53].

Therefore, evaluating the tunneling time in accordance with formula (1.6) leads to the emergence of supraluminal velocities and negative times in the FTIR theory. But these problems do not emerge when the tunneling time is associated with the group velocity v_g of waves in the barrier. By defining v_g in terms of the energy flux P and the energy density $W(z)$ in (2.6) and finding P and $W(z)$ for tunneling field (3.10), one can show that $v_g(z) = P/W(z) < c$ inside the barrier. The values of $v_g(z)$ for a nonuniform barrier are conveniently compared with the velocity of energy transfer in the field formed inside a uniform dielectric layer with a refractive index n_0 in the interference of the forward and backward waves. This velocity v_{g0} calculated in accordance with (2.6) depends on n_0 and is independent of z:

$$v_{g0} = \frac{2c}{1 + n_0^2}. \quad (3.16)$$

In the tunneling through a layer with the parameters $n_0 = 1.8$, $d = 80$ nm, $u^2 = 1.375$, and $y^2 = 1/3$ [49], the minimal velocity $v_g > v_{g0}$ and the maximum value of v_g is $1.5v_{g0}$. This ratio corresponds to the energy flux in the FTIR mode accelerated by 20–25% (in comparison with a uniform transparent layer).

In the foregoing, for simplicity of analysis, we considered the regime of FTIR in a substrate-free gradient layer. With the inclusion of the effect of a substrate, nonlocal dispersion effects remain in force, although the dependence on the substrate parameters complicates the formulas. In particular, the boundary conditions at the surface of a uniform substrate whose thickness is far greater than the tunneling

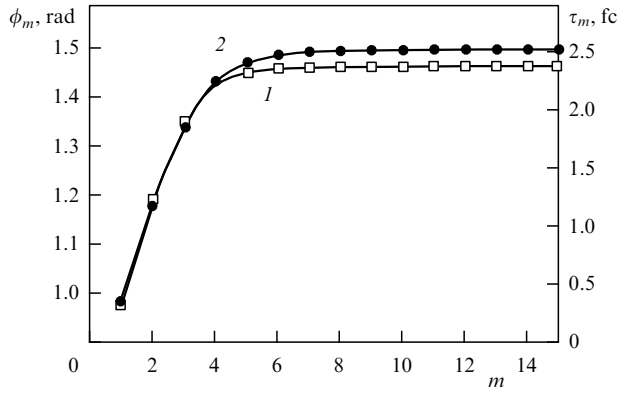

Figure 5. The phase ϕ_m (*1*) and the phase time τ_m (*2*) of a wave tunneling through a system of gradient layers (3.4) as functions of the number of layers m; $y^2 = 1/3$, $d = 80$ nm, and $n_{min} = 0.75n_0$.

pulse length and whose refractive index is n lead, instead of expression (3.10), to a different expression describing the contribution of the backward wave:

$$Q = -\frac{(in + n_1 + \gamma/2)\,\exp(-2p\eta_0)}{in + n_1 - \gamma/2}\,. \tag{3.17}$$

In this geometry, the reflection coefficient R is given by

$$R = \frac{(n + \gamma^2/4 + n_1^2)\,t - \gamma n_1 - i(n-1)\,(n_1 - \gamma t/2)}{(n - \gamma^2/4 - n_1^2)\,t + \gamma n_1 + i(1+n)(n_1 - \gamma t/2)}\,,$$

$$t = \tanh(mp\eta_0)\,. \tag{3.18}$$

For $n = 1$, formula (3.18) becomes formula (3.13).

As is evident from formula (3.18), the system of several gradient films (3.4) can be an efficient reflector. For example, we consider the case where the imaginary terms in the numerator of (3.18) vanish; this condition can be written as

$$x^2 = \frac{y^2 t^2}{1 + y^2}\,, \quad x = \sqrt{1 - u^{-2}}\,.$$

When this condition is satisfied, the reflection coefficient in (3.18) can be written as

$$R = \frac{nt^2 - (1 - t^2)\,n_1^2}{nt^2 + (1 - t^2)\,n_1^2}\,. \tag{3.19}$$

In particular, for a system of eight films ($y^2 = 1/3$, $d = 80$ nm, $n_0 = 1.8$), we obtain $R = 0.9993$; for a $\lambda = 800$ nm wave, the reflector under consideration is only 650 nm thick (without a substrate). *We emphasize an important property of this gradient reflector*: *its thickness is smaller than the wavelength*.

Along with the properties inherent in uniform photonic barriers, the effects of FTIR for barriers with a concave profile of the refractive index are noted for a feature associated with profile nonuniformity; this feature is considered in what follows.

4. Reflectionless wave tunneling in gradient optics

As noted above, the transmittance of a photonic barrier in FTIR systems decreases exponentially with the barrier width; the reflection of waves from the barrier becomes stronger and the reflection coefficient $|R|$ approaches unity. For a rectangular uniform barrier, this result follows directly from formula (2.2). Rapid attenuation of tunneling waves hinders observations of the FTIR effects.

But the reverse situation may also occur for some photonic barriers, when the interference of the forward and backward waves inside the barrier leads to the disappearance of reflection ($R = 0$) and, according to formula (3.13), to the total transmission ($|T| = 1$) of the tunneling wave energy flux. This situation occurs for a system of m gradient barriers with a concave profile of the refractive index. The condition for the occurrence of a reflection-free tunneling mode in such a system can be found by setting the expression for R in (3.13) equal to zero:

$$\tanh(mp\eta_0) = \frac{\gamma n_1}{1 + \gamma^2/4 + n_1^2}\,. \tag{4.1}$$

The phase of the wave at the output of the system is

$$\phi_t = \arctan\left(\frac{\gamma}{1 + n_1^2 - \gamma^2/4}\right). \tag{4.2}$$

To obtain the parameters of the optical system ensuring this regime from expression (4.1), we may specify, for instance, the values of n_0 and the parameter y that defines the modulation depth $n_{\max} = n_0\,(1 + y^2)^{-1}$.

We introduce a new variable $x = \sqrt{1 - u^{-2}}$ and, expanding γ in (3.7), rewrite Eqn (4.1) as [60]

$$\tanh(mxl_0) = \frac{2xy}{\sqrt{1 + y^2}}\left[\frac{1}{n_0^2} + \frac{y^2}{1 + y^2} + x^2\left(1 - \frac{1}{n_0^2}\right)\right]^{-1},$$

$$l_0 = \ln\left(\frac{y_+}{y_-}\right). \tag{4.3}$$

Solving this equation for x, we calculate the normalized frequency $u = \Omega/\omega$; for a given wave frequency ω, using expressions (3.9), we then find the layer thickness d that ensures the 100% transmittance ($|T|^2 = 1$) of the tunneling mode with the frequency ω. In particular, by choosing a material with $n_0 = 2.35$, we conclude that in a system of two barriers with the modulation depth $n_{\max} = 0.75 n_0$ ($y^2 = 0.33$), the condition $|T|^2 = 1$ is satisfied for $u = 1.1$. For example, this gives the width $d = 65$ nm for the wavelength $\lambda = 800$ nm and $d = 85$ nm for $\lambda = 1055$ nm. The transmission spectrum of these photonic barriers for tunneling waves ($u > 1$) is plotted in Fig. 6.

We emphasize that the effect under consideration is different from conventional reflection-free coatings in optical systems. It is known that a uniform transparent layer (with the thickness d and the refractive index n) does not reflect a wavelength λ if $nd/\lambda = \pi m/2$, where $m = 1, 2, 3, \ldots$; in this case, several frequencies for which $R = 0$ may appear in the transmission spectrum. By contrast, the gradient layer is opaque for all frequencies $\omega < \Omega$ and the condition $R = 0$ may be satisfied for only one frequency.

The amplitude and phase FTIR effects may occur not only in adjacent photonic barriers described by formulas (3.13)–(3.15) and (4.1), (4.2) but also in a system of barriers separated by a gap of finite width. For example, we consider the tunneling through two parallel dielectric layers (3.4) of thickness d separated by an air gap of width D (Fig. 7). To

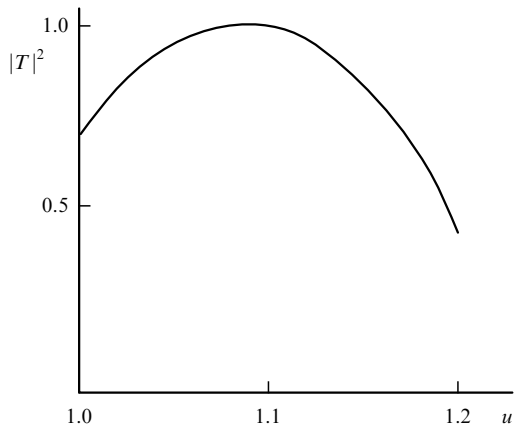

Figure 6. Transmission spectrum in the reflection-free wave tunneling through two layers ($n_0 = 2.35$, $d = 65$ nm, $y^2 = 1/3$).

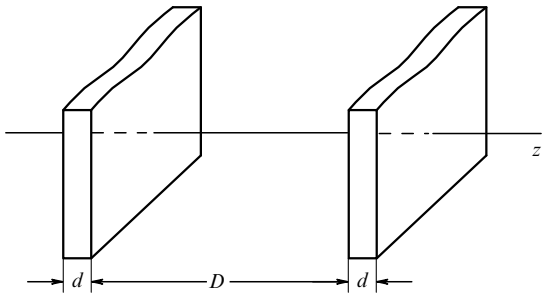

Figure 7. Setup for the observation of the generalized Hartman's effect in gradient layers of thickness d spaced at a distance D.

calculate the reflectivity R (3.12) of this system, the parameter Q_1 corresponding to the left layer must be expressed in terms of the parameters of the air gap and the right layer. Proceeding from right to left and consecutively using the field continuity conditions at the planes $z = 2d + D$, $z = d + D$, $z = d$, and $z = 0$, we obtain

$$Q_1 = \exp(-2p\eta_0) \times \frac{2n_1 Q_0 + \tan(kD)(1 + Q_0)\left[1 + S(n_1 - \gamma/2)\right]}{2n_1 + \tan(kD)(1 + Q_0)\left[1 - S(n_1 + \gamma/2)\right]}, \quad (4.4)$$

$$S = \frac{n_1(1 + Q_0)}{1 - Q_0} - \frac{\gamma}{2}. \quad (4.5)$$

The quantities Q_0 and n_1 are defined in (3.10) and (3.12). Substituting Q_1 given by (4.4) in expression (3.12), we find the reflection coefficient R of the entire system for an arbitrary distance D between the layers.

Also noteworthy is an important property of the quantity Q_1, which characterizes the backward wave in the left layer (see Fig. 7): when the distance D is an integer multiple of the half-wave,

$$D = \frac{s\lambda}{2}, \quad s = 1, 2, 3, \ldots, \quad \tan(kD) = 0, \quad (4.6)$$

formula (4.4) reduces to formula (3.10), which defines Q_1 for adjacent barriers. Therefore, in the case (4.6), the gap D has no effect on the amplitude or phase structure of the tunneling wave (the generalized Hartman effect [27, 28]). In particular, the reflection-free FTIR mode occurs for D is (4.6) as well as for $D = 0$, under condition (4.1).

Repeating this reasoning for m parallel layers shows that the phase 'saturation' seen in Fig. 7 occurs in the geometry of Fig. 7 for a large number of layers separated by arbitrarily wide gaps D in (4.6).

We also note that the optics of thin gradient films was considered above neglecting the effect of a substrate; but the results obtained remain valid when the thickness D of a transparent uniform nonabsorbing substrate satisfies condition (4.6), where λ is the wavelength in the substrate material.

When a narrow-band wave pulse of a finite duration t passes through photonic barrier (3.4) attached to a uniform substrate of thickness $d_1 \gg ct$ made of a material with a refractive index n_1, an FTIR mode with $R = 0$ occurs, as is evident from expression (3.18), if the following two conditions are simultaneously satisfied:

$$n_0 N_- = \frac{\gamma}{2}\tanh(ml_0 x), \; n_1 = \frac{n_0^2}{1 - x^2}\left(\frac{y^2}{1 + y^2} - x^2\right). \quad (4.7)$$

The parameter l_0 is defined in (4.3) and $x = \sqrt{1 - u^{-2}}$. For a given n_0, finding the value of x from the first equation in (4.7), it is possible to choose the value n_1 of the refractive index of the substrate to ensure reflection-free pulse tunneling. In particular, for $n_0 = 2.55$, $y^2 = 1/3$, and $x = 0.2$, Eqns (4.7) are satisfied for a system of two films ($m = 2$) with $n_1 = 1.42$ and $u = 1.02$. To make this system for a pulse of radiation with the wavelength $\lambda = 800$ nm requires films with a thickness $d = 120$ nm.

In the case of reflection-free tunneling ($|T| = 1$), the expression for the time τ_{Bu} in (1.7) reduces to simpler formula (1.6); however, the above-mentioned contradictions between the two definitions (τ and t_g) of the tunneling time in FTIR are retained in this case. For FTIR regimes in gradient photonic barriers, these contradictions are easily revealed for other wave types considered below. These problems for simple rectangular barriers (multilayer coatings [19] and subcritical waveguide sections [23]) are still under discussion; leaving this debatable issue open, we consider the reflection-free FTIR regimes that occur in gradient barriers inside a waveguide for waves of the radio-frequency region.

5. Microwave mode tunneling in waveguides

Microwave technology provides a convenient instrumental basis for experiments in FTIR because centimeters and nanoseconds — the spatio-temporal scales of the effects observed — are easier to measure than the corresponding short-scale quantities in optical tunneling. In particular, the first measurements of the transverse shift of rays in the total internal reflection (the Goos – Hanchen shift) were made for a beam of centimeter radio waves [49]. Measurements of the directivity of a horn antenna in the near-field region at the frequency 9.5 GHz [15] revealed anomalies of the group velocity v_g associated with the energy transfer in the emanating wave fields. These fields, localized in the air at distances 0.1 – 1 m from the antenna mouth center, may be treated as a peculiar kind of tunneling mode. The group velocity v_g of these modes, which was measured from the signal delay, exhibits a dependence on the angle between the horn axis and the radiation direction; in the directions close to the horn generatrix, the value of v_g amounted, according to the estimates in Ref. [15], to supraluminal values $1.2 - 1.4\,c$.

In another attempt to determine v_g of tunneling microwaves [6], a waveguide path with a stepwise narrowing of the waveguide cross section was used (Fig. 8, section *2*); the wave of the fundamental TE_{01} mode with a frequency ω propagated along the path between sections 1 and 3 (critical frequency Ω) experiencing the FTIR effect in section *2* (critical frequency Ω_{cr}), with $\Omega_{cr} > \omega > \Omega$. By measuring the time delay of the TE_{01} mode at the frequencies 9.45 GHz in the narrow section of the length 20 cm (critical frequency 9.494 GHz), the authors of Ref. [61] noted that their measurement data approached the τ_{Bu} values in model (1.7). The difficulties emerging in the pursuance of these experiments are associated with the exponential attenuation of the transmitted wave and the scattering of a part of its energy to higher-order modes at the ends of section 2.

Replacing the narrow waveguide section 2 (see Fig. 8) with a diaphragm made of a diamagnetic material with magnetic permeability $\mu < 1$ can furnish an alternative to this scheme [62]. The critical waveguide frequency in the diaphragm region is somewhat higher, which gives rise to the FTIR regime without changing the waveguide cross section,

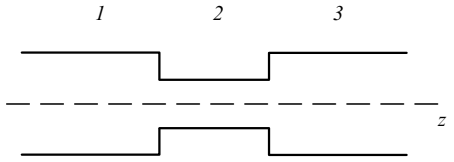

Figure 8. Microwave analog of FTIR in optics: narrowing of the waveguide profile (section *2*) for the tunneling of the fundamental mode between sections 1 and 3.

i.e., without losses due to the generation of higher-order modes. But the transmitted wave is then still attenuated in the course of tunneling. At the same time, both of the above loss mechanisms are eliminated when use is made of the effect of reflection-free tunneling considered in Section 4 for normal incidence. This requires replacing the waveguide narrowing by a diaphragm with a concave profile $\varepsilon(z)$ in (3.1), with the function $U^2(z)$ given by (see Fig. 4, profile *2*)

$$U^2(z) = 1 - \frac{1}{g} + \frac{W^2(z)}{g}\,, \quad W(z) = \left(\cos\frac{z}{L} + M\sin\frac{z}{L}\right)^{-1}. \tag{5.1}$$

The cross section of the waveguide path does not change in this geometry (Fig. 9), and the FTIR effect occurs due to nonlocal dispersion in the layer given by (5.1). In this model, the quantities $M > 0, g > 1$, and L are free parameters related to the thickness d of the layer described by (5.1) through the minimal value of the refractive index $n_{\min}$ and the profile slope angle δ near the boundary $z = 0$:

$$L = \frac{d}{\arcsin\left(2M/(1+M^2)\right)}\,,$$
$$n_{\min} = n_0\sqrt{1 - \frac{M^2}{g(1+M^2)}}\,, \quad \tan\delta = -\frac{2M}{gL}\,. \tag{5.2}$$

Therefore, unlike the model in (3.4), the concave-profile model in (5.1) involves an additional free parameter δ.

We again consider the fundamental TE_{01} mode, whose components E_x and H_y are expressed in terms of some auxiliary function Ψ in accordance with Eqns (3.2) and $H_z = -\partial\Psi/\partial y$ [51]; in this case, the equation $\operatorname{div}\mathbf{H} = 0$ is automatically satisfied and the function Ψ is described by the wave equation

$$\frac{\partial^2\Psi}{\partial z^2} + \frac{\partial^2\Psi}{\partial y^2} + \frac{(\omega n_0)^2 U^2}{c^2}\,\Psi = 0\,. \tag{5.3}$$

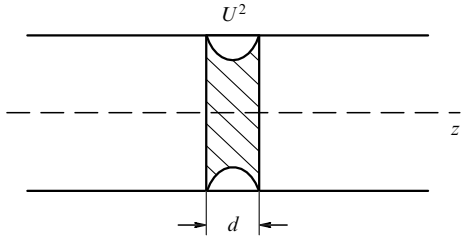

Figure 9. Schematic of the principal mode tunneling through a waveguide with a constant profile blocked by gradient dielectric diaphragms with the profile U^2 in (5.1).

For an empty waveguide ($n_0 = 1$, $U = 1$) of a rectangular cross section with sides a and b ($a > b$), the function Ψ is known:

$$\Psi = A\sin\left(\frac{\pi y}{b}\right)\exp\left[\mathrm{i}(\beta z - \omega t)\right],$$
$$\beta = \sqrt{\left(\frac{\omega}{c}\right)^2 - (k_\perp)^2}\,, \quad k_\perp = \frac{\pi}{b}\,. \tag{5.4}$$

To find the solution of Eqn (5.3) for the filled section of the waveguide $0 \leqslant z \leqslant d$, we can conveniently introduce a new variable u as

$$u = \ln\frac{1 + m_+\tan(z/2L)}{m_+ - \tan(z/2L)}\,,$$
$$m_+ = \sqrt{1+M^2} + M\,, \quad W(z) = \frac{\cosh u}{\sqrt{1+M^2}}\,. \tag{5.5}$$

Using this variable, the solution of Eqn (5.3) can be written as

$$\Psi = B\sqrt{\cos\frac{z}{L} + M\sin\frac{z}{L}}\,\sin\frac{\pi y}{b}\,F(u)\,\exp(-\mathrm{i}\omega t)\,. \tag{5.6}$$

In expressions (5.4) and (5.6), A and B are normalization factors. The function $F(u)$ in Eqn (5.6) is defined by the equation

$$\frac{\mathrm{d}^2F}{\mathrm{d}u^2} + F\left(q^2 - \frac{T}{\cosh^2 u}\right) = 0\,, \tag{5.7}$$
$$q^2 = \left(\frac{\omega n_0 L}{c}\right)^2\frac{1}{g(1+M^2)} - \frac{1}{4}\,,$$
$$T = L^2\left[\left(\frac{\omega n_0}{c}\right)^2\left(1 - \frac{1}{g}\right) - k_\perp^2\right] - \frac{1}{4}\,. \tag{5.8}$$

Equation (5.7) is quite often encountered in quantum mechanics [63] and its solutions are expressed in terms of hypergeometric functions in general. For simplicity, we here consider the special case $T = 0$; when $q^2 < 0$ in this case, Eqn (5.7) describes a tunneling wave. This situation occurs, for instance, for the TE_{01} mode with the frequency 10 GHz ($\omega = 2\pi\times 10^{10}$ rad^{-1}) in a waveguide of a rectangular cross section with the sides $a = 1$ cm and $b = 2$ cm for the diaphragm parameters $n_0 = 1.85$, $g = 2.25$, $M = 1.7$, $n_{\min} = 1.51$, and $d = 0.22$ cm; $q^2 = -0.177$. Introducing the parameter $p^2 = -q^2 > 0$, we conveniently represent the solution of Eqn (5.7) as the sum of forward and backward waves similar to solution (3.10):

$$F = \exp(-pu) + Q\exp(pu)\,, \quad p = \sqrt{-q^2}\,, \tag{5.9}$$
$$Q = \exp(-2pu_0)\,\frac{2p\sqrt{1+M^2} + M + 2\mathrm{i}\beta L}{2p\sqrt{1+M^2} - M - 2\mathrm{i}\beta L}\,, \quad u_0 = \ln m_+\,. \tag{5.10}$$

Using the field continuity conditions at the opaque layer boundaries $z = 0$ ($u = -u_0$) and $z = d$ ($u = u_0$), we then find the reflectivity of a system of m adjacent layers in a form similar to formula (3.13):

$$R = \frac{t_m\left[(\beta L)^2 + p^2(1+M^2) + M^2/4\right] - Mp\sqrt{1+M^2}}{t_m\left[(\beta L)^2 - p^2(1+M^2) - M^2/4\right] + Mp\sqrt{1+M^2} + \mathrm{i}\beta L\left(2p\sqrt{1+M^2} - Mt_m\right)}\,,$$
$$t_m = \tanh(2pmu_0)\,. \tag{5.11}$$

The condition $R = 0$, which corresponds to the 100% transmission of the tunneling TE_{01} mode, is satisfied for the diaphragm consisting of two layers with the parameters specified above ($2M = 1.7$, $g = 2.25$, $n_0 = 1.85$, $n_{\min} = 1.51$, and $d = 0.22$ cm). If the layer parameters are changed ($n_0 = 1.9$, $n_{\min} = 1.55$, and $d = 0.2$ cm) with the values of M and g unchanged, the condition $R = 0$ is satisfied for a diaphragm consisting of three layers. In these cases, the modulus of the transmission function is equal to 1 and the phase, defined by the formula

$$\phi_t = \arctan \frac{t_m\left[(\beta L)^2 - p^2(1+M^2) - M^2/4\right] + Mp\sqrt{1+M^2}}{\beta L\left(2p\sqrt{1+M^2} - Mt_m\right)} \tag{5.12}$$

that follows from formula (5.11), takes values close to $\pi/2$.

In comparing the FTIR effects in waveguides that arise from path narrowing (see Fig. 8) and from a gradient diaphragm (see Fig. 9), we also note several features of the wave barriers considered here.

(1) Recording of the tunneling TE_{01} mode in the geometry of Fig. 9 is not hindered by either the exponential attenuation of the wave or the generation of higher-order modes in scattering from the ends of the narrowing.

(2) The gradient diaphragm may be regarded as a device for shifting the phase of the wave without loss of its energy.

(3) Saturation of the wave phase with lengthening the tunneling path z (the insignificant change in the phase with increasing z from $z = 2d$ to $z = 3d$ shown above) expresses the Hartman effect for the gradient barrier. However, unlike conventional FTIR configurations, where the phase saturation is accompanied by a decrease in the transmittance $|T|$, the scheme considered shows that this decreasing effect is not universal for all FTIR schemes.

4. As noted in Ref. [23], the measurement data for the time of signal propagation through the narrowed waveguide are close to the τ_{Bu} values given by (1.7), which depend on $\partial \ln T/\partial\omega$; however, for a gradient diaphragm with $T = 1$, this derivative vanishes, which allows verifying this FTIR theory independently.

In connection with this possibility, we note Ref. [64]*, where measurements were made of the transmission spectrum in the region of gigahertz radio waves tunneling in a waveguide through a diaphragm made of a metamaterial: this spectrum corresponds to the case of total transmission* ($|T|^2 = 1$) *of the tunneling mode, which is due to the 'plasmon' transfer of wave energy in the diaphragm material* (*the effect previously noted in* Ref. [41]).

5. The phase ϕ_t of a wave tunneling in a waveguide across a diaphragm of thickness D may be larger than the wave phase increment $\Phi = \beta D$ over the same distance D in an empty waveguide. In particular, in the aforementioned case $R = 0$ for the TE_{01} mode, $\phi_t = \pi/2$, while $D = 2d$ and $\Phi = 0.61$ rad. By exciting this mode in a system of two similar waveguides, one of which contains a gradient diaphragm for FTIR, it is easy to see that the phase difference between the waves at the system output is equal to $\Delta\phi$; in the case under discussion, $\Delta\phi = 0.96$ rad. Such a microwave system is similar to a two-photon interferometer in optics [18]. By finding the phase ϕ_t from the measured $\Delta\phi$ and comparing the formation time of ϕ_t ($t_1 = \Phi/\omega$) with the phase time τ in (1.6) and the time t_g defined by the group velocity of the tunneling waves, it is possible to estimate the effectiveness of competing FTIR theories.

6. FTIR effects in a transmission line with continuously distributed parameters

Long transmission lines with continuously distributed parameters are characterized by the values of linear capacitance C and inductance L. In particular, for a strip line with the strip width a and interstrip spacing d, the quantities C and L are [58]

$$C = \frac{\varepsilon_0 \varepsilon a}{d}, \quad L = \frac{\mu_0 \mu d}{a}, \tag{6.1}$$

where $\varepsilon_0 = 8.85 \times 10^{-12}$ F m^{-1} and $\mu_0 = 4\pi \times 10^{-7}$ H m^{-1} are the permittivity and magnetic permeability of the vacuum, and ε and μ are the values of these parameters in the medium. When C and L retain constant values equal to C_0 and L_0 along the length of the line, the signal speed v_0 and the impedance Z_0 of the line are

$$v_0 = \frac{1}{\sqrt{L_0 C_0}}, \quad Z_0 = \sqrt{\frac{L_0}{C_0}}. \tag{6.2}$$

The current I and voltage V distributions in a loss-free line with distributed parameters satisfy the equations [51]

$$\frac{\partial V}{\partial z} + L\frac{\partial I}{\partial t} = 0, \quad \frac{\partial I}{\partial z} + C\frac{\partial V}{\partial t} = 0. \tag{6.3}$$

In the framework of system of equations (6.3), we consider the case where the capacitance or inductance distributions are nonuniform, for instance, the distribution of C in the section $0 \leqslant z \leqslant d$ depends on the z coordinate:

$$C(z) = C_1 U^2(z), \quad U(0) = U(d) = 1. \tag{6.4}$$

By introducing an auxiliary function Ψ with the help of the relations

$$V = -L_0\frac{\partial \Psi}{\partial t}, \quad I = \frac{\partial \Psi}{\partial z}, \tag{6.5}$$

we obtain an equation that coincides with wave equation (3.3) after the replacement $c/n_0 \to v_0$. In this case, representations (6.5) for V and I are analogous to representation (3.2) for the electric and magnetic components of the wave field.

By extending this analogy, it is possible to investigate a strip line with the capacitance modulation of form (3.4) and (3.5), produced, for instance, by a smooth variation of $\varepsilon(z)$ with unchanged geometrical dimensions a and d. In this case, a cutoff frequency Ω occurs in the nonuniform strip line, related to the velocity v_0 as

$$\Omega = \frac{2v_0 y\sqrt{2+y^2}}{d}. \tag{6.6}$$

In the subcritical case $\omega < \Omega$, the voltage and current waves, which are described by the function Ψ_t in (3.10), tunnel through the line section $0 \leqslant z \leqslant d$. The wave reflection coefficient for the modulated capacitance section and the condition for reflection-free tunneling through this section are given by formulas (3.13) and (4.3) with the replacement $n_0^2 \to C_0/C_1$. Therefore, the tunneling of current and voltage waves in a transmission line with continuously distributed parameters exhibits similarities to FTIR effects in gradient optics.

Continuous modulation of parameters permits imparting new properties to a long line:

(i) waveguide-type frequency dispersion characterized by a controllable cutoff frequency;

(ii) the possibility of matching line sections that is unrelated to their geometrical dimensions;

(iii) control of the phase of the transmitted wave without power loss in the FTIR regime, when the phase shift depends on the modulation parameters rather than the path length.

Despite the formal similarity to the effects of gradient thin-film optics, we must draw a significant physical distinction between these systems: the refractive index of a film $n_0 > 1$, while the corresponding parameter $(C_0/C_1)^{1/2}$ for a transmission line in formulas (3.13) and (4.3) may be either greater or smaller than unity. This correspondence furnishes the possibility of flexible modeling of tunnel effects in transmission lines with continuously distributed parameters. Similar possibilities for a line with a transient capacitance $C(t)$ are demonstrated in Ref. [59].

7. Gradient optics of surface waves

In the foregoing, we considered wave tunneling through nonuniform media in the direction of the gradient of the refractive index n (see Section 3) or, in the more general case, at an angle to this direction (see Section 5). In this case, the wave field structure is determined by tunneling in the grad n direction and by the propagation in the direction perpendicular to grad n. In the vicinity of the boundary of a nonuniform medium, this field corresponds to a surface wave; the tunneling causes the field to decrease on either side of the boundary, and its amplitude and phase structure depends on the profile of the refractive index in the near-boundary layer of the medium.

To emphasize the peculiarity of these fields, they are conveniently compared to surface waves at an abrupt interface of two uniform dielectrics. The polarization and spectrum of these waves traveling in the y direction along the interface (the $z = 0$ plane) are known [65]:

(i) the wave field involves the E_y, E_z, and H_x components (the TH polarization); the TE-polarized surface wave (the H_y, H_z, and E_x components) is impossible in this system, although such waves have been noted for other media, in particular for photorefractive materials [66] and antiferromagnets [67];

(ii) the surface wave at the interface of uniform media is impossible when the permittivities of these media satisfy the condition $\varepsilon_1 + \varepsilon_2 < 0$. This implies that the permittivity of at least one medium must satisfy the condition $\varepsilon < 0$; this situation is possible, for instance, in the solid-state plasma of a metal or a dielectric with free carriers [68];

(iii) the frequency spectrum of surface waves at the interface of the air and the plasma of a solid with the plasma frequency $\Omega_{\rm pl}$ is bounded from above: $\omega < \Omega_{\rm pl}/\sqrt{2}$.

However, in contrast to TH waves, another field structure of a surface wave is possible for a smooth variation of the profile $\varepsilon(z)$. This variation is conveniently considered in the framework of the exactly solvable model given by (5.1), in which $W(z) = (1 + z/L)^{-1}$, $z \geqslant L$. A dependence of this type describes the 'saturation' $\varepsilon(z) = n_0^2 U^2(z)$ deep in the medium ($z \gg L$), where the refractive index takes the bulk value n_v:

$$n(z=0) = n_0\,, \quad n(z \gg L) = n_0\sqrt{1-\frac{1}{g}} = n_v\,, \quad g > 1\,. \tag{7.1}$$

In model (7.1), the TE-polarized surface wave is possible at the boundary between a nonuniform dielectric and the air ($W = 1$). The E_x, H_y, and H_z components of this wave field are conveniently expressed in terms of the generating function Ψ defined by wave equation (5.3). By representing the Ψ function in the form [69]

$$\Psi = A\sqrt{W} f(u)\,\exp\left[\mathrm{i}(k_y y - \omega t)\right], \quad u = 1 + \frac{z}{L}\,, \tag{7.2}$$

we use Eqn (5.3) to obtain the Bessel equation for the function $f(u)$:

$$\frac{\mathrm{d}^2 f}{\mathrm{d}u^2} + \frac{1}{u}\,\frac{\mathrm{d}f}{\mathrm{d}u} + f\left(p^2 - \frac{s^2}{u^2}\right) = 0\,, \tag{7.3}$$

$$p^2 = \left(\frac{\omega}{c}\right)^2 (n_v^2 - b^2) = -p_1^2\,, \quad s^2 = \frac{1}{4}\left(1 - \frac{\omega^2}{\Omega_{\rm cr}^2}\right),$$

$$b = \frac{ck_y}{\omega}\,, \quad \Omega_{\rm cr} = \frac{c}{2L\sqrt{n_0^2 - n_v^2}}\,. \tag{7.4}$$

The solutions of Eqn (7.3) that decay with the z coordinate are the modified Bessel functions $K_s(p_1 L u)$. These solutions, which occur for $p^2 < 0$ $(p_1^2 > 0)$ and $s^2 > 0$, describe the structure of a field localized in the nonuniform medium at the $z = 0$ boundary; in this case, $n_v^2 < b^2$.

The generating function in the region $z \leqslant 0$ is given by

$$\Psi_1 = B\exp\left[\frac{z}{l} + \mathrm{i}\,(k_y y - \omega t)\right], \tag{7.5}$$

where l is the characteristic field localization scale length in the region $z < 0$, and A and B are the normalization factors of solutions (7.2) and (7.5). The field continuity conditions at the boundary $z = 0$ permit relating the constants A and B to the characteristic lengths l and L:

$$B = AK_s(p_1 L)\,, \tag{7.6}$$

$$\frac{L}{l} = \frac{1}{2} + p_1 L\,\frac{\mathrm{d}K_s}{\mathrm{d}u}\,K_s^{-1}\,. \tag{7.7}$$

We expand the function $K_s(p_1 L)$ in a series in the domain of small values of the argument $[(p_1 L)^2 \ll 1]$ and keep the first term of the expansion to rewrite Eqn (7.7) in the form

$$\frac{L}{l} = \frac{1}{2} - s + \ldots\,. \tag{7.8}$$

Because the derivative of the decreasing function K_s is negative and $L/l > 0$, we obtain a restriction for the index of the Bessel function K_s: $0 < s < 1/2$.

To find the dispersion equation of the surface wave under discussion, we note that the dimension l of its localization in the air is related to the frequency ω by the equation $b^2 = 1 + (c/l\omega)^2$ following from expression (7.5). In this case, $b = ck_y/\omega > 1$, and hence the wavenumber of the surface wave is greater than the value of k_y for a wave of the same frequency ω in empty space $z < 0$. The above surface wave may be excited by increasing the projection k_y of the wave incident from the $z < 0$ domain. For this, we can use a scheme resembling FTIR in the configuration of Fig. 1 if the wave, on passing the prism with a refractive index $n_{\rm pr}$ and a gap, impinges on the surface of gradient medium (7.1) instead of the second prism [70, 71]. The dimensionless parameter b in expression (7.4) is then given by $b = n_{\rm pr}\sin\theta$, and therefore

the condition $b > n_v$, which is required for field attenuation inside the medium, may be satisfied. In Eqn (7.8), we express the attenuation length l in terms of the parameter b to obtain the dispersion equation for the TE surface wave:

$$\frac{b^2-1}{n_0^2-n_v^2}=\left(\frac{v}{1\pm\sqrt{1-v^2}}\right)^2, \quad v=\frac{\omega}{\Omega_{\rm cr}}. \tag{7.9}$$

Here, $v \leqslant 1$ is the normalized frequency of surface waves, and the critical frequency $\Omega_{\rm cr}$ is defined in (7.4). The wave spectrum given by (7.9) contains two branches, which merge at the point $v = 1$; to each frequency v, there formally correspond two values of $b = n_{\rm pr}\sin\theta$, but only one of these values is compatible with the condition $b > n_v$ in (7.4) for realistic parameters of the problem. The same situation persists when the next term of the expansion of K_s is substituted in Eqn (7.8):

$$K_s(p_1L)=-s+\frac{(p_1L)^2}{2(1-s)}\ldots. \tag{7.10}$$

In approximation (7.10), corrections to the b values found from Eqn (7.9) do not exceed several percent.

We note that the critical density $\Omega_{\rm cr}$ in (7.4) varies over a wide spectral range comprising the IR, near-IR, and even visible parts of the spectrum, depending on the near-surface layer parameters n_1, n_v, and L. In particular, for a gradient dielectric with $n_0 = 1.57$, $n_v = 1.55$, and $L = 70$ nm, the frequency $\Omega_{\rm cr}$ is equal to 8.08×10^{15} rad s^{-1}. Surface TE waves with the frequency $\omega = 2.69\times10^{15}$ rad s^{-1} ($\lambda = 700$ nm), which are close to the red edge of the visible spectrum, and TE waves with $\omega = 3.22\times10^{15}$ rad s^{-1} ($\lambda = 585$ nm), which represent the center of the visible region, may propagate along the boundary of this medium in accordance with Eqn (7.9). The incidence angles for $n_{\rm pr} = 1.9$ are respectively equal to 71.3° and 57.3° for the above waves with $\lambda = 700$ nm and $\lambda = 585$ nm.

The above TE waves at the boundary of a gradient medium differ in the mechanism of field penetration into the medium from the TH waves at an abrupt interface: the TH waves tunnel, as noted above, in the medium where $\varepsilon < 0$, while the TE waves tunnel in the medium where $\varepsilon > 0$, but $\partial\varepsilon/\partial z < 0$. A transition layer of finite thickness is required for the existence of the TE waves; with broadening of this layer ($L \to \infty$), the critical frequency decreases to zero, the nonuniformity vanishes ($U = 1$, $n_0 = n_v$), and Eqn (7.9) transforms into the trivial condition $n\sin\theta = 1$ for the total internal reflection of incident waves.

We also note some features of TE surface waves arising from their tunneling across a thin ($L < \lambda$) near-boundary layer with decreasing permittivity:

(1) The critical frequency $\Omega_{\rm cr}$ in (7.4) is not related to the density of free carriers in the medium, and these waves can therefore propagate along the boundaries of solids void of free carriers; this property substantially broadens the range of materials that allow the use of TE surface waves.

(2) The high values of $\Omega_{\rm cr}$, which are defined by the nonlocal dispersion of a gradient layer, permit extending the frequency spectrum of TE surface waves towards both the short- and long-wavelength parts of the spectrum.

(3) The losses due to TE surface wave attenuation may be optimized by choosing the gradient material whose absorption bands are located away from the wave frequencies in use.

8. Conclusion. Two-dimensional problems of the FTIR theory

To conclude, we briefly discuss new and insufficiently elaborated problems of wave tunneling: curvilinear photonic barriers, the role of absorption, optomechanical effects, transient problems, and, above all, polarization tunneling effects.

1. The difference in the FTIR modes for S- and P-polarized waves arises when they are obliquely incident on the surface of a gradient barrier. To generalize the corresponding results obtained in Sections 3 and 4 for normal incidence to the case of an arbitrary angle requires a more complicated analysis involving hypergeometric functions. We present some of the results of this analysis without derivation [72].

We consider wave incidence at an arbitrary angle θ onto a gradient layer of thickness d, whose refractive index $n(z)$ increases from the value n_0 at the layer center ($z = 0$) to the value $n_{\max} > n_0$ at the boundaries $z = \pm d/2$:

$$n=n_0U(z), \quad U(z)=\left(\cos\frac{z}{L}\right)^{-1}, \quad \frac{n_{\max}}{n_0}=\left(\cos\frac{d}{2L}\right)^{-1}. \tag{8.1}$$

In this model, S-wave propagation through a layer with refractive index (8.1) is characterized by a nonlocal dispersion and the cutoff frequency Ω, which is caused by layer nonuniformity:

$$\Omega=\frac{c\arccos M}{n_0d}, \quad M=\frac{n_0}{n_{\max}}. \tag{8.2}$$

For a layer with the parameters $d = 80$ nm and $n_0 = 1.4$, the cutoff frequency $\Omega = 1.25\times10^{15}$ rad s^{-1} lies in the near-IR range ($\lambda = 1500$ nm). S waves with frequencies $\omega < \Omega$ propagate across this layer in the FTIR regime. However, P waves of the same frequency incident at the same angle pass through this layer in the ordinary regime, not experiencing the tunnel effect. Therefore, nonuniformity (8.1), which defines nonlocal wave dispersion, is additionally responsible for the barrier birefringence of a sort that underlies the fundamental difference in transmission of the S and P waves.

Polarized-wave transmission spectra at oblique wave incidence as functions of the dimensionless parameter γ are shown in Fig. 10:

$$\gamma=1-\frac{\sqrt{1-u^{-2}}}{2}, \quad u=\frac{\Omega}{\omega}>1. \tag{8.3}$$

The properties of these spectra are noteworthy:

(i) a narrow transmission peak ($|T|^2 = 1$, reflection-free tunneling) for S waves;

(ii) steep downward excursions of $|T_{\rm S}|^2$ near the cutoff frequency $u = 1$ and of $|T_{\rm P}|^2$ in the region $u \geqslant 3$;

(iii) a high contrast ratio between $|T_{\rm S}|^2$ and $|T_{\rm P}|^2$; the ratio $\chi = |T_{\rm S}|^2/|T_{\rm P}|^2$, which characterizes this contrast, ranges down to $\chi < 0.05$ or up to $\chi > 90$ in narrow spectral intervals.

As is evident from Fig. 10, the gradient layer under discussion can be of interest in the development of narrow-band frequency filters and polarizers [73] operating at rather large incidence angles $b^2 = 1 + (c/l\omega)^2$. The influence of the substrate (the $|T_{Sn}|^2 = 1$ curve) smears the peak of $|T_{\rm S}|^2$, although the peak $|T_{\rm S}|^2 = 1$ itself, like the properties (ii) and (iii), also manifests itself in the presence of a substrate; insignificant substrate-induced distortions of the P-wave transmission spectrum are not shown in Fig. 10. When the

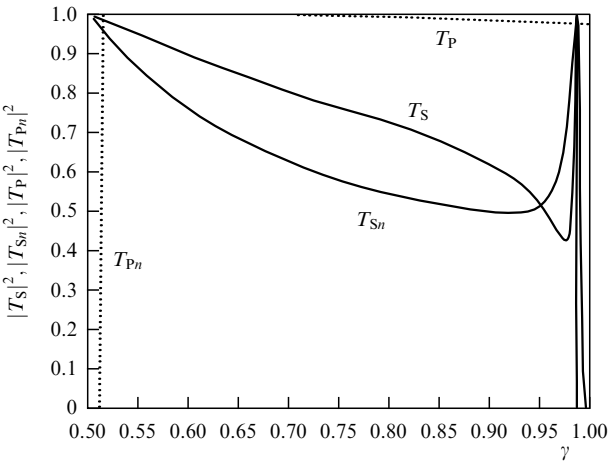

Figure 10. Transmission spectra for tunneling S waves ($|T_S|^2$) and propagating P waves ($|T_P|^2$) for a gradient layer (8.1), $d = 80$ nm, $n_0 = 1.4$, and $M = 0.85$; $\theta = 65°$, the parameter γ is defined by expression (8.3), the peak $|T_S|^2 = 1$ corresponds to reflection-free S-wave tunneling. The curve $|T_{Sn}|$ represents the effect of a substrate on the S-wave transmission.

layer parameters n_0 and M in (8.2) and the angle θ are known, formulas (8.3) allow finding the layer thickness d that ensures the S- and P-wave transmission mode characterized by the given value of $\gamma(u)$ for a given wavelength λ:

$$\frac{d}{\lambda} = \frac{\sqrt{1 - 4(1-\gamma)^2}\,\arccos M}{2\pi n_0}\,. \tag{8.4}$$

In particular, under the conditions corresponding to Fig. 10, for $|T_S|^2 = 1\,(\gamma = 0.985)$, for instance, we obtain the ratio $d/\lambda = 0.09$ corresponding to a thin-layer filter for S waves.

2. Quite often considered in connection with losses in bent light guides is the tunneling through cylindrical barriers [74]; in particular, parasitic modes of the 'whispering gallery' type may emerge for a small bending radius. For a light guide with a core of thickness d, an external radius of its rounding r_0, and refractive indices of the core and the cladding n_1 and $_2$, the condition for the emergence of such a mode is given by $d/r_0 > (n_1 - n_2)/n_2$ [75].

For spherical photonic barriers, reflection and transmission spectra were discussed in connection with the ray orbiting effect emerging in the scattering of waves from concentric dielectric spheres [76]. The analysis of similar effects for continuous radial distributions of the refractive index $n(r)$ is fraught with considerable mathematical difficulties even for simple power-law $n(r)$ dependences [77].

3. The monotonic saturation of the phase of a tunneling wave was discussed above for a conservative medium. It was noted in Ref. [48] that the absorption in the gradient layer material lowers the rate of saturation, and the phase variation becomes periodic for a sufficiently strong absorption. The reflection and transmission of waves tunneling through an absorbing gradient layer with a complex permittivity $\varepsilon = \operatorname{Re}\varepsilon + \mathrm{i}\operatorname{Im}\varepsilon$, $\operatorname{Re}\varepsilon > 0$, may be investigated with the help of formula (3.13) with the replacements

$$\begin{aligned} &t_m \to S\,, \quad n_1 \to n_0(a - \mathrm{i}b)\,, \quad a - \mathrm{i}b = \sqrt{u^2 - 1 - \mathrm{i}\zeta}\,,\\ &\zeta = \frac{\operatorname{Im}\varepsilon}{\operatorname{Re}\varepsilon}\,, \quad S = \frac{t_1 + \mathrm{i}t_2}{1 - \mathrm{i}t_1 t_2}\,, \quad t_1 = \tanh\frac{pa\eta_0}{c}\,,\\ &t_2 = \tan\frac{pb\eta_0}{c}\,, \quad p = \frac{\omega n_0}{c}\,, \quad n_0 = \sqrt{\operatorname{Re}\varepsilon}\,. \end{aligned} \tag{8.5}$$

At the same time, a conservative gradient layer deposited on an absorbing substrate can make up an FTIR configuration, giving rise to quenching of the reflected wave (reflection-free coating of the absorber [69]).

4. Optomechanical effects of nanoparticle capture and entrainment in the fields of tunneling waves were noted in Refs [78 – 80]; controllable displacement of the closely spaced sections of optical fibers under the action of outgoing modes, which is of interest for microphotonics problems, was considered in Ref. [81].

5. In the foregoing, we noted an analogy between the stationary FTIR effects in quantum mechanics and optics described by solutions of the stationary Schrödinger and Helmholtz equations. This analogy is easily seen in the simple case where the permittivity profile in Helmholtz equation (3.3) is of the form $U^2(z) = C - V(z)$, where C is a constant; in this case, Eqn (3.3) for a monochromatic wave coincides with the Schrödinger equation, where C is the particle energy and $V(z)$ is the external potential. However, for the $U^2(z)$ profiles in (3.4) or (5.1), Helmholtz equation (3.3) is brought to the form of the Schrödinger equation only by special transformations of variables $\eta = \eta(z)$ in (3.8) and (5.5). It is precisely these transformations that allow revealing the important role of nonlinear dispersion in the optics of gradient media.

In tunneling across barriers with a time-dependent height, this analogy breaks down: in quantum mechanics, such effects are described by transient solutions of the Schrödinger equation dependent on the first time derivative $\partial\Psi/\partial t$, and in optics, by solutions of the wave equation containing the second derivative $\partial^2\Psi/\partial t^2$. The special character of transient FTIR is discussed in Ref. [82] by the example of the EM wave passage across a barrier whose height oscillates in time; the tunneling through a moving barrier was considered in Ref. [83]. An interesting application of the transient FTIR concept was proposed in Ref. [84], where the penetration of individual Bose-condensate atoms through the walls of an optical trap is treated as the tunneling of matter waves. Comparison of the investigation of stationary and transient FTIR processes shows that the latter have only recently come under close scrutiny, however.

To conclude, there is good reason to mention the prospects of using wave tunneling effects both in applied problems of gradient nanooptics (thin-film filters and polarizers, reflectors, and reflection-free coatings) and in the solution of basic problems related to optimization of the energy transfer by waves of different spectral regions. Another important field is taking shape in the generalization of optical FTIR effects to nonlocal quantum mechanical electron tunneling through potential barriers [6, 8, 13]. The common nature of the FTIR concepts for different wave fields is also beginning to attract attention in the analysis of particle dynamics in atomic physics [85, 86].

Acknowledgements. The author is grateful to T Arecci, V Kuzmiak, A Migus, G Petite, L Stenflo, and S Haroche for their interest in this work and the stimulating criticism.

References

1. Gamow G *Z. Phys.* **51** 204 (1928)
2. Condon E U, Morse P M *Rev. Mod. Phys.* **3** 43 (1931)
3. MacColl L A *Phys. Rev.* **40** 621 (1932)
4. Wigner E P *Phys. Rev.* **98** 145 (1955)
5. Hartman T E *J. Appl. Phys.* **33** 3427 (1962)
6. Hauge E H, Støvneng J A *Rev. Mod. Phys.* **61** 917 (1989)

7. Chiao R Y, Steinberg A M, in *Progress in Optics* Vol. 44 (Ed. E Wolf) (Amsterdam: Elsevier, 2002) p. 143
8. Muga J G, Leavens C R *Phys. Rep.* **338** 353 (2000)
9. de Fornel F *Evanescent Waves: from Newtonian Optics to Atomic Optics* (Springer Ser. in Opt. Sci., Vol. 73) (Berlin: Springer, 2001)
10. Winful H G *Phys. Rev. Lett.* **90** 023901 (2003)
11. Büttiker M, Washburn S *Nature* **422** 271 (2003)
12. Olkhovsky V S, Recami E, Jakiel J *Phys. Rep.* **398** 133 (2004)
13. Enders A, Nimtz G *J. Phys. I* (France) **2** 1693 (1992)
14. Nimtz G, Enders A, Spieker H *J. Phys. I* (France) **4** 565 (1994)
15. Brodowsky H M, Heitmann W, Nimtz G *Phys. Lett. A* **222** 125 (1996)
16. Ranfagni A et al. *Phys. Rev. E* **48** 1453 (1993)
17. Mugnai D, Ranfagni A, Ronchi L *Phys. Lett. A* **247** 281 (1998)
18. Steinberg A M, Kwiat P G, Chiao R Y *Phys. Rev. Lett.* **71** 708 (1993)
19. Laude V, Tournois P *J. Opt. Soc. Am. B* **16** 194 (1999)
20. Feynman R P, Hibbs A R *Quantum Mechanics and Path Integrals* (New York: McGraw-Hill, 1965)
21. Büttiker M *Phys. Rev. B* **27** 6178 (1983)
22. Büttiker M, Landauer R *J. Phys. C: Solid State Phys.* **21** 6207 (1988)
23. Ranfagni A et al. *Appl. Phys. Lett.* **58** 774 (1991)
24. DeWitt-Morette C, Foong S K *Phys. Rev. Lett.* **62** 2201 (1989)
25. Ranfagni A et al. *Phys. Rev. E* **63** 025102 (2001)
26. Gaveau B et al. *Phys. Rev. Lett.* **53** 419 (1984)
27. Olkhovsky V S, Recami E, Salesi G *Europhys. Lett.* **57** 879 (2002)
28. Longhi S et al. *Phys. Rev. E* **65** 046610 (2002)
29. Nimtz G, Heitmann W *Prog. Quantum Electron.* **21** 81 (1997)
30. Chiao R Y *Phys. Rev. A* **48** R34 (1993)
31. Chiao R Y et al. *Quantum Semiclass. Opt.* **7** 279 (1995)
32. Aharonov Y, Erez N, Reznik B *Phys. Rev. A* **65** 052124 (2002)
33. Azbel' M Ya *Solid State Commun.* **91** 439 (1994)
34. Shaarawi A M, Besieris I M *J. Phys. A: Math. Gen.* **33** 7255 (2000)
35. Ziolkowski R W *Phys. Rev. E* **63** 046604 (2001)
36. Milonni P W *J. Phys. B: At. Mol. Opt. Phys.* **35** R31 (2002)
37. Moritz E *Mol. Cryst. Liquid Cryst.* **41** 63 (1977)
38. Musielak Z E, Fontenla J M, Moore R L *Phys. Fluids B* **4** 13 (1992)
39. Xu K, Zheng X, She W *Appl. Phys. Lett.* **85** 6089 (2004)
40. Krekora P, Su Q, Grobe R *Phys. Rev. A* **63** 032107 (2001)
41. Pendry J B *Phys. Rev. Lett.* **85** 3966 (2000)
42. Greisukh G I, Bobrov S T, Stepanov S A *Optics of Diffractive and Gradient-Index Elements and Systems* (Bellingham, Wash.: SPIE Opt. Eng. Press, 1997)
43. Yeh P *Optical Waves in Layered Media* (New York: Wiley, 1988)
44. Heavens O S *Optical Properties of Thin Solid Films* (New York: Dover Publ., 1991)
45. Lee S-J et al. *Appl. Phys. Lett.* **82** 2133 (2003)
46. Grigorenko A N et al. *Nature* **438** 335 (2005)
47. Ginzburg V L *Zh. Eksp. Teor. Fiz.* **34** 1593 (1958) [*Sov. Phys. JETP* **7** 1096 (1958)]
48. Shvartsburg A B, Petite G *Eur. Phys. J. D* **36** 111 (2005)
49. Haibel A, Nimtz G, Stahlhofen A A *Phys. Rev. E* **63** 047601 (2001)
50. Li C-F, Wang Q *J. Opt. Soc. Am. B* **18** 1174 (2001)
51. Griffiths D J *Introduction to Electrodynamics* (Upper Saddle River, NJ: Prentice Hall, 1999)
52. Lee B, Lee W *J. Opt. Soc. Am. B* **14** 777 (1997)
53. Petrillo V, Refaldi L *Opt. Commun.* **186** 35 (2000)
54. Muga J G et al. *Phys. Rev. A* **66** 042115 (2002)
55. Longhi S *Phys. Rev. E* **64** 037601 (2001)
56. Chiao R Y, Kozhekin A E, Kurizki G *Phys. Rev. Lett.* **77** 1254 (1996)
57. Wang L J, Kuzmich A, Dogariu A *Nature* **406** 277 (2000)
58. Balcou Ph, Dutriaux L *Phys. Rev. Lett.* **78** 851 (1997)
59. Shvartsburg A, Petite G, in *Progress in Optics* Vol. 44 (Ed. E Wolf) (Amsterdam: Elsevier, 2002) p. 123
60. Shvartsburg A B, Petite G *Opt. Lett.* **31** 1127 (2006)
61. Ranfagni A et al. *Phys. Scripta* **42** 508 (1990)
62. Martin Th, Landauer R *Phys. Rev. A* **45** 2611 (1992)
63. Landau L D, Lifshits E M *Kvantovaya Mekhanika: Nerelyativistskaya Teoriya* (Quantum Mechanics: Non-Relativistic Theory) (Moscow: Fizmatlit, 2001) [Translated into English: 3rd ed. (Oxford: Pergamon Press, 1977)]
64. Baena J D et al. *Phys. Rev. B* **72** 075116 (2005)
65. Landau L D, Lifshits E M *Elektrodinamika Sploshnykh Sred* (Electrodynamics of Continuous Media) (Moscow: Nauka, 1992) [Translated into English (Oxford: Pergamon Press, 1984)]
66. Cronin-Golomb M *Opt. Lett.* **20** 2075 (1995)
67. Youfa W, Qi W, Jiashan B *J. Appl. Phys.* **84** 6233 (1998)
68. Raether H *Surface Plasmons on Smooth and Rough Surfaces and on Gratings* (Springer Tracts in Modern Physics, Vol. 111) (Berlin: Springer-Verlag, 1988)
69. Shvartsburg A, Petite G, Auby N *J. Opt. Soc. Am. B* **16** 966 (1999)
70. Otto A *Z. Phys.* **216** 398 (1968)
71. Kretschmann E *Z. Phys.* **241** 313 (1971)
72. Shvartsburg A, in *Nonlinear Waves: Classical and Quantum Aspects* (NATO Sci. Ser., Ser. II, Vol. 153, Eds F Kh Abdullaev, V V Konotop) (Dordrecht: Kluwer Acad. Publ., 2004) p. 389
73. Macleod H A *Thin-Film Optical Filters* 3rd ed. (Bristol: Institute of Physics Publ., 2001)
74. Wu L et al. *Photonics Nanostruct. Fundam. Appl.* **1** 31 (2003)
75. Marcuse D *Theory of Dielectric Optical Waveguides* 2nd ed. (Boston: Acad. Press, 1991)
76. Nussenzveig H M *Diffraction Effects in Semiclassical Scattering* (Cambridge: Cambridge Univ. Press, 1992)
77. Ramakrishna S A, Pendry J B *Phys. Rev. B* **69** 115115 (2004)
78. Okamoto K, Kawata S *Phys. Rev. Lett.* **83** 4534 (1999)
79. Chaumet P C, Rahmani A, Nieto-Vesperinas M *Phys. Rev. Lett.* **88** 123601 (2002)
80. Ng L N et al. *Appl. Phys. Lett.* **76** 1993 (2000)
81. Büttiker M, Landauer R *Phys. Rev. Lett.* **49** 1739 (1982)
82. Pimpale A, Holloway S, Smith R J *J. Phys. A: Math. Gen.* **24** 3533 (1991)
83. Steck D A, Oskay W H, Raizen M G *Science* **293** 274 (2001)
84. Povinelli M L et al. *Opt. Lett.* **30** 3042 (2005)
85. León J *J. Phys. A: Math. Gen.* **30** 4791 (1997)
86. Aquilera-Navarro V C, Iwamoto H, de Aquino V M *Int. J. Theor. Phys.* **43** 483 (2004)